Reversed-phase high-performance liquid chromatography using enhanced-fluidity mobile phases

Yi Cui, Susan V. Olesik*

Department of Chemistry, The Ohio State University, 120 West 18th Avenue, Columbus, OH 43210, USA

Abstract

The use of enhanced-fluidity liquids in reversed-phase HPLC separations is characterized. Enhanced fluidity liquids are commonly used liquids with high proportions of low viscosity fluids, such as carbon dioxide, added. When carbon dioxide is added to the methanol–water mobile phase, substantially lower plate heights and time of analysis are achieved without losing mobile phase solvent strength. The results indicate that these improvements are caused by the combination of the increased diffusivity of the enhanced-fluidity solvents and the ability of carbon dioxide to readily break hydrogen bonds in the methanol–water mixtures.

1. Introduction

High-performance liquid chromatography (HPLC) is often used to separate non-volatile compounds. However, HPLC does have limitations. HPLC typically has longer analysis times and lower efficiencies than supercritical fluid chromatography (SFC). The primary cause of these deficiencies is the low rate of diffusion in liquids compared to that in supercritical fluids. Liquids have diffusion coefficients on the order of 10^{-5} cm²/s compared to $10^{-4} - 10^{-3}$ cm²/s for supercritical fluids. Yet, SFC is incapable of separating highly polar compounds.

We previously showed that liquid mobile phases with enhanced fluidity could provide HPLC some of the advantages of SFC, such as decreased time of analysis without losing a significant advantage of liquids which is high solvent strength [1]. To produce these enhanced-

fluidity solvents, large proportions of low viscosity liquids are dissolved in common eluents used for HPLC. The previous work was a demonstration of the advantage of using methanol–CO_2 mixtures as the eluent in porous glassy carbon HPLC.

In this paper, we describe the use of enhanced-fluidity solvents in reversed-phase HPLC. The most common eluents used in HPLC are mixtures of water with methanol or acetonitrile. There are substantial drawbacks to the use of methanol–water mixtures as eluents. The methanol–water mixture viscosity is larger than that of the components. For example, at 50% (w/w) methanol (or 0.56 mole ratio methanol–water), the mixture viscosity is approximately twice the viscosity of water [2]. In addition, high viscosities will lower efficiencies and increase the time of analysis. This paper describes the use of methanol–water–carbon dioxide mixtures as eluents for reversed-phase HPLC. We hypothesized that the addition of substantial portions of carbon dioxide to the mixture would decrease

---

* Corresponding author.

the mixture viscosity without affecting the solvent strength substantially.

2. Theory

The theory involved in the use of enhanced-fluidity solvents in HPLC was described in detail previously [1]. The details pertinent to reversed-phase separations are reviewed herein. In reversed-phase liquid chromatography the predominant contribution to band dispersion is commonly diffusion in the stagnant mobile phase inside the porous packing. Using the Knox equation [3], the C term, that describes the non-equilibrium between the mobile phase and the stationary phase, is a function of capacity factor, k', and an inverse function of D_m, the diffusion coefficient of the analyte in the mobile phase and $u_{min} \propto D_m/[f(k')]^{1/2}$. If by lowering the viscosity, the diffusion coefficients of the solutes can be increased without a substantial increase in k', then the time of analysis should decrease and efficiency should increase in reversed-phase separations by addition of carbon dioxide to the mobile phase.

The mobile phase system chosen for analysis includes a constant methanol–water mole ratio of 2.3 with carbon dioxide added to it in proportions that varies from 0 to 0.5 mole fraction. This methanol–water mixture is commonly used as an eluent in isocratic HPLC separations and its viscosity is approximately 1.5 times that of water [2]. Three polynuclear aromatic hydrocarbons (PAHs), naphthalene, phenanthrene and pyrene were used as test analytes.

2.1. Analyte diffusion coefficients

Two models were used to predict the binary diffusion coefficients of the analytes in these enhanced fluidity mixtures, the modified Wilke–Chang [4] (Eqs. 1 and 2) and Perkins–Geankoplis [5] (Eq. 3). Both theories have been successful in predicting diffusion coefficients in mixed liquids.

$$D_{Am} = 7.4 \cdot 10^{-8} \cdot \frac{(\phi M)^{1/2} T}{\eta_m V_A^{0.6}} \qquad (1)$$

$$\phi M = \sum (x_i \phi_i M_i) \qquad (2)$$

where D_{Am} is the diffusion coefficient of solute A in mixture m, η_m is the mixture viscosity, V_A is the molar volume of solute A at its normal boiling temperature, T is temperature, x_i is mole fraction, ϕ_i is the Wilke–Chang association constant of solvent component i and M_i is molecular mass of solvent component i.

$$D_{Am}\eta_m^{0.8} = \sum x_i D_{Ai}\eta_i^{0.8} \qquad (3)$$

where x_i is mole fraction of i in the mixture; η_i is the viscosity of pure i and D_{Ai} is the diffusion coefficient of A in pure component i. The viscosities of the methanol–water–CO_2 mixtures (Fig. 1) were calculated using the Teja–Rice method [6–8]. The viscosities of methanol and water were corrected for operating pressures using the estimation technique of Lucas [9]. Literatures values of the viscosity of CO_2 at various pressures were used [10]. The accuracy of the viscosity predictions using the pressure-modified Teja–Rice method was estimated by comparison with experimentally measured viscosities of methanol–CO_2 mixtures [1]. The
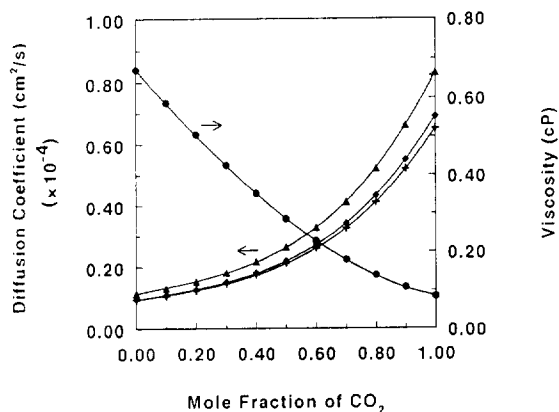

Fig. 1. Calculated diffusion coefficients of naphthalene (▲), phenanthrene (◆), pyrene (+), and viscosities (●) of methanol–water–CO_2 mixtures at 25°C and 204 atm with methanol–water mole ratio held at 2.3.

viscosity predictions were within 5% of the experimental values.

To evaluate the accuracy of each model for predicting the diffusion coefficients of solutes in enhanced-fluidity liquids, experimental diffusion coefficients of methanol–CO_2 mixtures [11] were compared to the predictions. The predicted diffusion coefficients were within 5% of the experimental values. Fig. 1 shows the predicted average diffusion coefficients for the analytes as a function of solvent composition calculated using Eqs. 1–3. The calculated diffusion coefficient of naphthalene varied from $1.2 \cdot 10^{-5}$ to $2.7 \cdot 10^{-5}$ cm^2/s when the mole fraction of CO_2 varied from 0 to 0.5.

3. Experimental

3.1. Column preparation

A packed capillary column containing Adsorbosphere octadecyl polysiloxane-coated 5-μm silica particles with 80 Å pore size (Alltech, Deerfield, IL, USA) was used in this study. The column was prepared by slurry packing the particles in acetonitrile with 1% Triton X-100 surfactant (Aldrich, Milwaukee, WI, USA) [12]. The ODS particles were held in the fused-silica column with a microbore end-fitting (U-434, Upchurch Scientific, Oak Harbor, WA, USA) that contained a 2-μm frit (C407 ×, Upchurch Scientific). The ODS slurry was placed in a 15 cm × 5 mm I.D. stainless-steel tube (used as a reservoir) and then pushed into a 30 cm × 320 μm I.D. fused-silica tube (Polymicro Technologies, Phoenix, AZ, USA). The pressure was increased gradually up to approximately 300 atm (1 atm = 101 325 Pa), then maintained at that pressure for at least 2 h. The column was depressurized overnight by turning off the pump and allowing the whole system to gradually approach atmospheric pressure.

3.2. Chromatographic system

The chromatographic system used in this study was similar to that used in the previous study of enhanced-fluidity HPLC [1]. The instrumentation included an ISCO (Lincoln, NE, USA) LC-2600 syringe pump, a Valco (Houston, TX, USA) W-series high-pressure injection valve with an internal injection volume of 60 nl, and a Spectroflow 757 UV–Vis absorbance detector (Kratos, Ramsey, NJ, USA). The detector wavelength was 254 nm. The end of the chromatographic column was connected with a zero-dead-volume fitting to a piece of 100-μm I.D. fused-silica tubing. The polyimide coating was removed from a 5-mm length of this tubing to create the detection cell. A 5- or 10-μm I.D. fused-silica restricting tube was placed after the detector to control the linear velocity in the column. As in SFC, the flow restrictor is a necessary part of the chromatographic system. Additionally, in enhanced-fluidity HPLC, the column pressure must be maintained above a minimum pressure to avoid having the mobile phase mixture separate into two phases (liquid–gas). For example, for 0 and 0.5 mole fractions of CO_2 the necessary column outlet pressures were 61 and 82 atm, respectively [13]. The column inlet pressure was maintained at 204 atm throughout the study. Sodium nitrite, methylene chloride and acetone were considered as possible non-retained markers. The retention times of all three compounds were the same across the whole mixture composition range. Acetone was used as the non-retained marker because the concentration needed to provide an observed response was least.

3.3. Materials

The analyte test mixture was a methanol solution containing 0.4 mg/ml naphthalene and 0.5 mg/ml each of phenanthrene and pyrene. All solvents and analytes were obtained from Aldrich with purity levels of ≥98%. Supercritical fluid-grade CO_2 was obtained from Scott Specialty Gases (Plumsteadville, PA, USA). Methanol–water–CO_2 mixtures were prepared by using two syringe pumps. A 2.3 mole ratio mixture of methanol and water of a given volume was placed in a syringe pump. The liquid CO_2 was maintained at 272 atm and room

temperature in another syringe pump. From the known density of CO_2 under these conditions, the requisite volume of CO_2 was added to the methanol–water mixture in the other syringe pump to make a given solution composition. The final solution was pressurized to 204 atm, and equilibrated at 25°C for at least 12 h.

3.4. Data collection and analysis

An IBM-AT-compatible computer was used for all data collection and analysis. The chromatograms were collected at a sampling rate of 10 points/s using a DT2821 12-bit, 50 kHz analog-to-digital converter (Data Translations, Marlboro, MA, USA). Data analysis was accomplished by using original programs written in the ASYST programming environment (Keithley Data Acquisition Div., Taunton, MA, USA). Post-run analysis included calculation of the zeroth, first and second statistical moments of a given chromatographic band. The second statistical moment was used to determine the experimental plate heights. A Gaussian peak of known variance was overlayed onto the experimental chromatographic band to allow visual confirmation of the second statistical moment.

4. Results and discussion

4.1. Evaluation of column bed quality

Before the properties of reversed-phase separations using enhanced-fluidity mobile phases were determined, the integrity of the column bed was evaluated. The flow resistance parameter, φ, is often used to evaluate the quality of the packing structure in the chromatographic column. The flow resistance parameter is defined as:

$$\varphi = \frac{\Delta P t_0 d_p^2}{\eta L_c^2} \qquad (4)$$

where ΔP is the pressure drop along the column, t_0 is the dead time of the column, d_p is the packing particle diameter, η is the eluent viscosi-

ty and L_c is the column length. A well-packed column of spherical particles should have a φ value between 500 and 1000 [14]. Higher values of the flow resistance parameter are indicative of crushed packing or the presence of too many fines in the column packing. The slurry-packed ODS column with the 2.3 mole ratio mixture of methanol and water as mobile phase had a flow resistance parameter of 775 which is well within the acceptable range for a well-packed column. Fig. 2 shows the variation of the flow resistance parameter with mobile phase composition. The flow resistance parameter decreased with increased percent CO_2 in the mobile phase.

Another characteristic which is commonly used to evaluate columns is the total porosity, ϵ_T, which is defined as the following equation:

$$\epsilon_T = \frac{F_v t_0}{r_c^2 L_c \pi} \qquad (5)$$

where F_v is the volumetric flow-rate and r_c is the column radius. With a mixture of water and methanol, the slurry-packed ODS column had a total porosity, $\epsilon_T = 0.723$. The total porosity is the sum of the column interparticle porosity, ϵ_u, and intraparticle porosity, ϵ_i. Estimates of ϵ_u and ϵ_i can be determined by non-chromatographic methods, e.g. mercury porosimetry. However, porosities measured with Hg may not accurately represent the pore structure observed by the
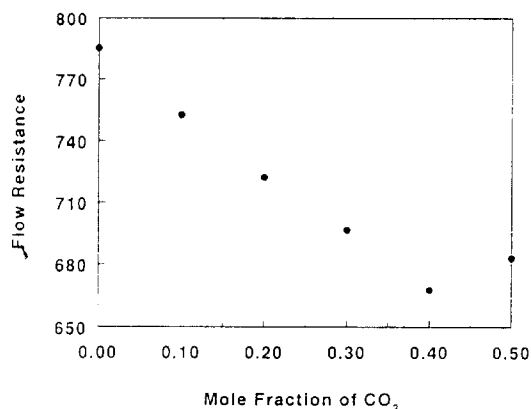

Fig. 2. Dependence of the flow resistance on mole fraction of CO_2 in the mobile phase with methanol–water mole ratio held at 2.3.

analytes in the column. The column interparticle porosities were determined with the modified Kozeny–Carman equation [15]:

$$\varphi = 180\psi^2 \cdot \frac{(1 - \epsilon_u)^2 \epsilon_T}{\epsilon_u^3} \tag{6}$$

where ψ^2 is a structural factor which is equal to 1 for spherical packing [15]. The intraparticle porosity was then determined by difference, $\epsilon_T - \epsilon_u$. Both experimental values of interparticle porosity, $\epsilon_u = 0.394$, and intraparticle porosity, $\epsilon_i = 0.329$ correspond well with those reported by other groups for similar well-packed ODS columns [15–17].

4.2. Retention

The expected gains in chromatographic efficiency and lowering of the analysis time is predicated on the assumption that the capacity factor will not increase significantly with added carbon dioxide. Fig. 3 shows the change in the capacity factors (k') versus the mole fraction of added CO_2 in the mobile phase. For all three analytes, the retention decreased with added CO_2. From 0–0.3 mole fraction CO_2 in the mobile phase, capacity factors decreased 38, 51 and 54% for naphthalene, phenanthrene and pyrene, respectively. However, over the range of
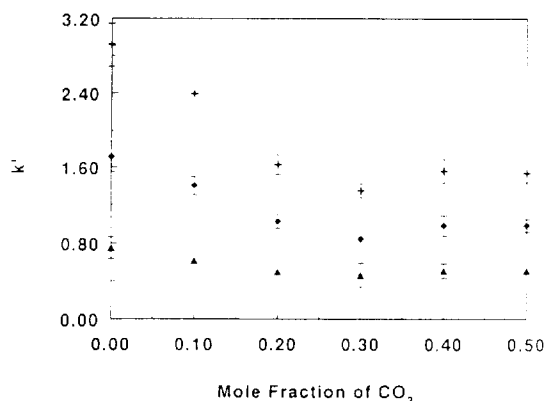
0.3–0.50 mole fraction CO_2, the analyte retention remained fairly constant.

4.3. Solvent strength measurement

To better understand the eluent strength of the methanol–water–CO_2 mixtures a study of solvent strength variation with added CO_2 was undertaken. Kamlet–Taft solvatochromic parameters, π^*, α and β were measured for the mixed methanol–water–CO_2 eluent (Fig. 4). The specific details of the solvatochromic measurements were described in a previous work [1]. These methods are also similar to those used by Kamlet et al. [18] and Cheong and Carr [19]. Both π^* and α decrease slowly when the percentage of CO_2 in the mobile phase increased, while β increased with added CO_2.

In a previous publication [1], we measured the solvent strength variation that occurred when 0 to 100% carbon dioxide was added to methanol. The addition of carbon dioxide had negligible effect on the measured α and β values until more than 60% carbon dioxide was added and for CO_2 concentrations higher than 60%, the observed decrease in the α and β parameters was similar. The minimal change in the hydrogen-bond acidity or basicity was believed to be caused by carbon dioxide functioning as a struc-
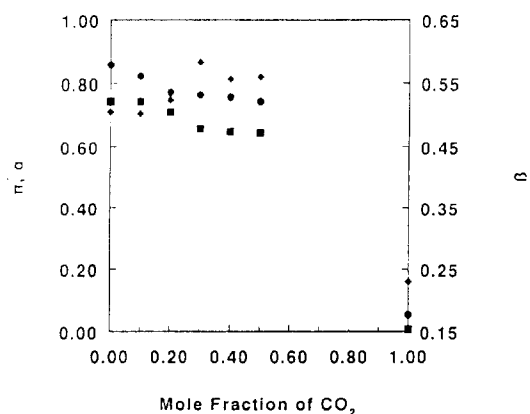

Fig. 3. Variation of capacity factors with mole fraction of CO_2 in the mobile phase when the methanol–water mole ratio is held at 2.3. ▲ = Naphthalene; ◆ = phenanthrene; + = pyrene.

Fig. 4. Variation of experimentally measured Kamlet–Taft parameters with mole fraction of CO_2 in the mobile phase when the methanol–water mole ratio is held at 2.3. The standard error for π^* (■), α (●) and β (◆) are ± 0.02, ± 0.06 and ± 0.04, respectively.

ture breaker, lowering the extent of self-associa-tion in methanol and therefore maintaining the hydrogen-bond acidity and basicity of the mix-ture. In the same methanol–CO_2 mixture, the π^* value decreased by approximately 50% over the 0–60% CO_2 composition range. The solvent strength variation in the methanol–water–CO_2 system is much different with added CO_2 than the methanol–CO_2 system. α and π^* decrease by approximately 10% over the range of 0–0.5 mole fraction CO_2 and the β value increases with added CO_2. Also a marked increase in H-bond basicity is observed between 0.2 and 0.40 mole fraction of added CO_2. Liquid CO_2 has solvent strength parameters of $\alpha = 0.05$, $\pi^* = 0.07$ and $\beta = 0.23$ at 170 atm and 25°C (Fig. 4). Again the CO_2 is decreasing the hydro-gen-bond association in the solvent. Otherwise the solvent strength would decrease montonically with added CO_2. Methanol ($\beta = 0.62$) is a much stronger H-bond base than CO_2 or water ($\beta = 0.18$). Therefore monomeric methanol is proba-bly being released from hydrogen-bond self-as-sociation or methanol–water hydrogen-bond as-sociation to cause the observed increase in H-bond basicity.

Sadek et al. [20] first showed that solute hydrogen-bond basicity and to a lesser extent solute dipolarity were important in establishing retention behavior in reversed-phase separations using ODS. Increases in the hydrogen-bond basicity and dipolarity of solutes lead to de-creased retention. Solute hydrogen-bond acidity variation did not seem to impact the measured retention. Accordingly, changing to mobile phases with decreased acidity should also cause decrease solute retention because of expected increased affinity of the solutes for the mobile phase.

The observed decrease in α over the same eluent composition region where the substantial decrease in retention occurs may mean that solvent hydrogen-bond acidity is important in controlling the retention in this reversed-phase ODS system similar to what Sadek et al. [20] described in their system. However, solvent polarity is not the only factor typically involved in the retention of PAH compounds on reversed-phase stationary phases. The shape or structure

of the stationary phase also affects the retention of PAH molecules [21,22]. We show later in this paper that the ordering of the stationary phase or mobile phase is also substantially affected by the addition of CO_2 to the eluent.

4.4. Chromatographic efficiency

The separation of naphthalene, phenanthrene and pyrene was complete for all of the mobile phase compositions studied. The column ef-ficiency was measured using an eluent composi-tion that varied from 0 to 0.5 mole fraction CO_2 with the mole ratio of methanol–water main-tained at 2.3. The inlet pressure was maintained at 204 atm, and temperature was maintained at 25°C throughout these measurements. The maxi-mum mobile phase velocity was limited by the minimum pressure necessary to keep the eluent mixture one phase at the end of the column. As described in the Experimental section, with increasing proportions of CO_2 in the mobile phase, higher post-column pressure was neces-sary. Therefore, the maximum possible linear velocity decreased with added CO_2. As Fig. 5 shows, linear velocities higher than typically used in HPLC were readily achieved with the chosen experimental conditions. If higher linear veloci-ties than those in Fig. 5 are desired, this can be readily achieved by increasing the column inlet pressure. We chose however to standardize the study by maintaining the column inlet pressure at 204 atm.

Fig. 5 illustrates the variation in the reduced plate height versus reduced velocity for the three analytes under different mobile phase composi-tions. Each data point is an average of 2–3 values to ensure the precision of the results. Using Eq. 7, these values were also corrected for the band dispersion contribution caused by the connecting tubing which included the detector volume (see Experimental section).

$$\sigma_{\mathrm{T}}^2 = \frac{\pi^2 r_{\mathrm{T}}^6 L_{\mathrm{T}} u_{\mathrm{T}}}{24 D_{\mathrm{m}}} \tag{7}$$

σ_{T}^2 is the connecting tube volumetric variance, r_{T} is the tube radius, L_{T} is the tube length, u_{T} is the linear velocity within the tube, and D_{m} is the
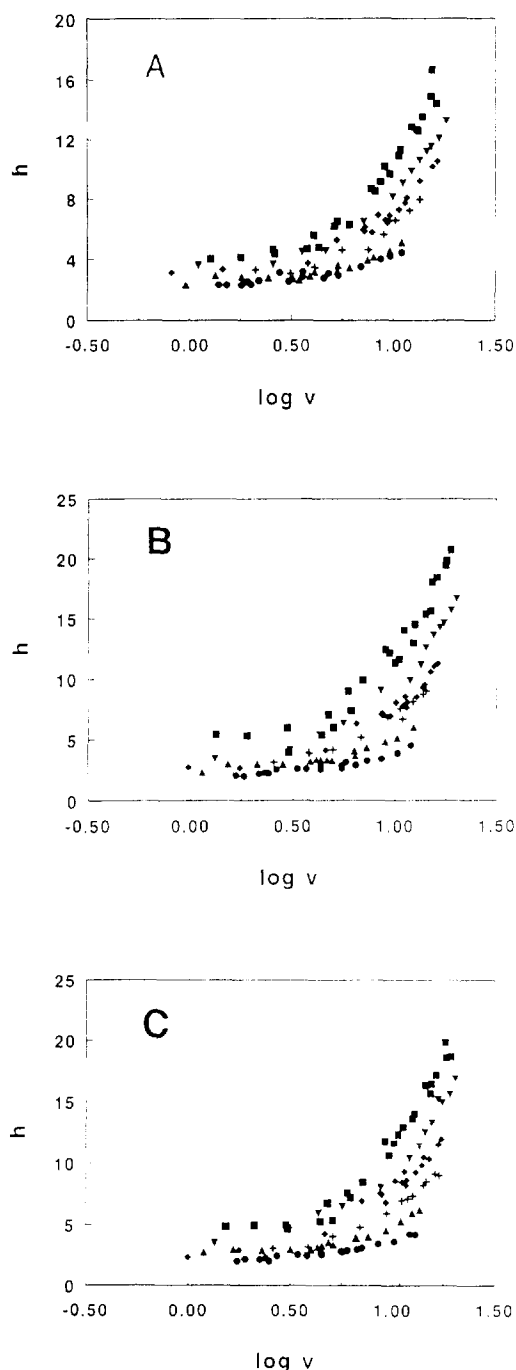
Fig. 5. Reduced plate height (h) of (A) naphthalene, (B) phenanthrene and (C) pyrene vs. reduced linear velocity (ν). ■ = methanol–water; ▼ = 0.1 CO_2 mole fraction; ◆ = 0.2 CO_2 mole fraction; + = 0.3 CO_2 mole fraction; ▲ = 0.4 CO_2 mole fraction; ● = 0.5 CO_2 mole fraction in the methanol–water–CO_2 mobile phase when the methanol–water mole ratio is held at 2.3.

solute binary diffusion coefficient. The contribution to band dispersion caused by the interconnecting tubing caused 2% error in the band dispersion at the lowest linear velocities and 5% error at the highest velocity studied. Other extracolumn sources of error contributed <1%. No effort was taken to correct the measured peak widths for such small errors. The curves for all three analytes are very similar. With increasing CO_2 in the eluent, the reduced plate height decreased across the entire velocity range studied. However, the decrease in plate height was marked at high velocities. For example, at a reduced velocity of 2, the reduced plate height for naphthalene changed from 4 (or $H = 0.02$ mm) to 2 (or $H = 0.01$ mm) for a change in eluent composition of 0 to 0.5 mole fraction CO_2; however for a reduced velocity of 10, the reduced plate height for naphthalene decreased from 11 to 4 for the same eluent composition change.

To better understand the chromatographic band dispersion process involved in this system the data in Fig. 5 were fit to the Knox equation [3]. The Knox equation is defined as:

$$h = A\nu^{1/3} + B/\nu + C\nu \tag{8}$$

where h is the reduced plate height and ν is the reduced linear velocity. $A\nu^{1/3}$ describes the band dispersion from flow anisotropy in the mobile phase and $C\nu$ describes the band dispersion caused by mass transfer between the mobile and stationary phases. B/ν describes the dispersion caused by axial molecular diffusion, and it contributes to the total band dispersion only when ν is smaller than 2. When the B term was included in the fitting equation, it was found to be statistically insignificant because the low-velocity region was not sampled in this study. Therefore the final equation used to fit the experimental data included only the flow anisotropy and mass transfer terms at $\nu > 2$. All the fitted equations had coefficients of correlation for the fits, $r \geqslant 0.95$. Fig. 6 shows the change in coefficients A and C with added CO_2 in the mobile phase.

Typical values of the constant A for a well packed column are approximately 1. A values greater than 2 or 3 indicate a poorly packed
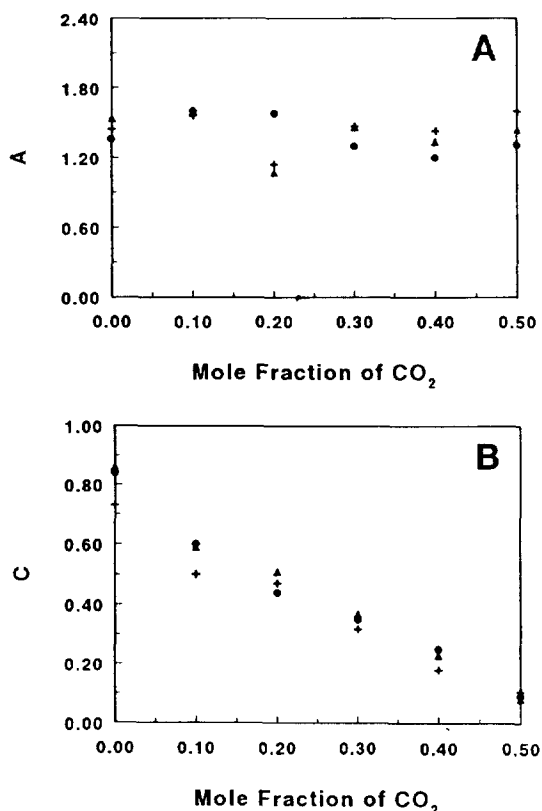
Fig. 6. Variation of (A) flow anisotropy, A term and (B) mass transfer resistant, C term with mole fraction of CO_2 in the mobile phase when methanol–water mole ratio is held at 2.3. The average standard errors for the A and C terms are $\pm$ 0.1 and $\pm$ 0.04, respectively.

column [3,23]. For all three analytes, the constant A varied from 1–1.5 with no trend with composition change observed. The last constant in the Knox equation is the C term, the sum of resistance to mass transfer and the kinetics of analyte desorption from the stationary phase. In Fig. 6B, the C terms of all three analytes are plotted versus the mole fraction CO_2 in the mobile phase. With no added CO_2, the C values are approximately 0.75–0.85. Karlsson and Novotny [24] recently reported a C value of 0.37 for a 265-μm I.D. capillary column packed with 5-μm ODS coated silica particles. They also showed that the value of the measured C term increased with the internal diameter of the microcolumn. The internal diameter of the column used in this study was larger, 320 μm.

However, it is highly doubtful that this small difference in column internal diameter would cause the C value to double. A more logical cause of the differences in the measured C values is the different mobile phases used in each study. Karlsson and Novotny used acetonitrile–water and we used methanol–water. The viscosity difference between the mixture and the pure components is much larger for the methanol–water mobile phase than in the acetonitrile–water mobile phase. In addition, as more CO_2 was added to the methanol–water system, the C terms for all the analytes decreased dramatically to values as low as $C = 0.08$ for naphthalene with 0.5 mole fraction CO_2. The C terms also did not vary significantly among the analytes studied which indicates that the trend in C term was not caused by capacity factor variation.

The most likely causes of the large C coefficient with the methanol–water mobile phase include: unaccounted extra-column band broadening such as injection profile, column quality, or slow kinetics associated with the reversible binding of the PAH compounds by the stationary phase. We believe the primary cause of the large C coefficient is slow kinetics. Using the theoretical model of Karger et al. [25], the band dispersion caused by the injection profile was calculated to be less than 1% of the total measured variance and was therefore considered negligible. The quality of the column was documented early in this paper and other results that are described later will further substantiate its integrity.

Eq. 9 is the relationship derived by Horváth and Lin [26,27] which describes the dispersion in the stagnant mobile phase inside the pores of the particles (C_{stag}) and the kinetics of desorption at the stationary phase (C_{kin}).

$$C = C_{stag} + C_{kin}$$
$$= \frac{\theta(k_0 + k' + k_0 k')^2}{30 k_0 (1 + k_0)^2 (1 + k')^2}$$
$$+ \frac{2k' D_m}{(1 + k_0)(1 + k')^2 d_p^2 k_d} \cdot \nu \qquad (9)$$

D_m is the diffusion coefficient of the analyte in a

given solvent, θ is the tortuosity factor for the porous packing and k_0 is the ratio of the intraparticulate void volume to the interstitial void space in the column (which can be experimentally determined from the intraparticular and interstitial porosities), k_d is the desorption rate constant and d_p is particle diameter of the column packing. Using our experimental data and Eq. 9 the band broadening caused by diffusion in the stagnant mobile phase of the pores was predicted. Then this value was subtracted from the total C value to provide an estimate of the proportion of the band broadening caused by slow desorption kinetics, C_{kin}. The estimated diffusion coefficients described previously were then substituted into the expression for C_{kin} to allow the calculation of an approximate k_d. This calculation was used to show the order of magnitude changes in the rate constant. Table 1 shows the variation of the desorption rate constant as a function of added CO_2 to the mobile phase. The rate constant increased significantly with added CO_2.

The plate height contribution caused by slow desorption kinetics is inversely related to the desorption rate constant and the particle size. Horváth and Lin [27] predicted significant band dispersion contributions from kinetic resistance for ODS particle sizes less than 6 μm. Others have also reported the significance of kinetic resistance in reversed-phase HPLC [28]. However, the cause of the low desorption rate was not discussed. When methanol–water mobile phases are used, the evidence below indicates the major cause of slow desorption kinetics is the formation of a polar hydrogen-bonded layer of water or water–methanol on the stationary phase surface. When increasing quantities of CO_2 are added to the methanol–water eluent, structure breaking of the hydrogen-bonded layer occurs and the desorption rate constant increases.

Fig. 7 shows data that supports this hypothesis. β-Naphthol and naphthalene have similar capacity factors across the entire eluent composition range. For example, for the eluent with methanol–water mole ratio of 2.3, the capacity factors of naphthalene and β-naphthol were 0.75 and 0.28, respectively. However, the reduced plate height of each chromatographic band was different as shown in Fig. 7. The slope of the β-naphthol curve, which mainly represents the effect of the C term contributions, is smaller than that of naphthalene. The hydroxyl on β-naphthol may allow ready movement of naphthol

Table 1
Calculation of rate constants of the desorption kinetics

Analyte	Mole fraction of CO_2	Calculated C_{stag}	Observed C (i.e., $C_{stag} + C_{kin}$)	Calculated k_d (s^{-1})
Naphthalene	0.00	0.091	0.73	19
	0.10	0.084	0.50	32
	0.20	0.077	0.47	37
	0.30	0.075	0.31	70
	0.40	0.078	0.17	209
Phenanthrene	0.00	0.12	0.86	13
	0.10	0.11	0.59	24
	0.20	0.10	0.51	34
	0.30	0.095	0.37	59
	0.40	0.10	0.23	152
Pyrene	0.00	0.14	0.84	11
	0.10	0.13	0.60	21
	0.20	0.12	0.44	40
	0.30	0.11	0.35	65
	0.40	0.11	0.25	137
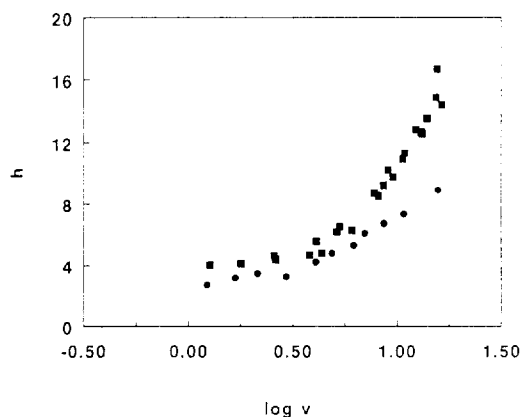
Fig. 7. Plots of reduced plate height (h) of naphthalene ($\blacksquare$) and naphthol ($\bullet$) vs. reduced linear velocity (ν) when methanol–water mixture was used as mobile phase.

through the structured layer above the ODS phase; while naphthalene has more difficulty.

Our hypothesis of the existence of the hydrogen-bonded surface layer that is broken by increasing proportions of carbon dioxide is also compatible with the predominance of other published information in stationary phase composition, structure and polarity. Yonker et al. [29] proposed a ternary component model of the stationary phase that was composed of a combination of silica substrate, bonded organic moiety and solvated layer consisting of mobile phase components. For the methanol–water composition used in our study, Yonker et al. [29] proposed a "brush"-like solvated stationary phase structure in which the C_{18} chains become erect and minimal intermolecular interactions between individual chains occurs. Also at this composition, the individual C_{18} chains were believed to be highly solvated by the methanol in the system which resulted in liquid-like motion of the C_{18} chains and partitioning into the chain structure as part of the retention mechanism. However, more recent NMR studies of ODS motion in methanol–water solutions comparable to those used herein shows that the ODS chain motion under these conditions is highly hindered. Gangoda and Gilpin [30] showed that the ^{13}C NMR spectrum of ODS solvated with a methanol–water (60:40, v/v) mixture (0.67 mole ratio), was

very similar to that of unsolvated ODS. This was contrasted to the NMR spectrum of ODS solvated with pure methanol which had line shapes that were liquid-like. If a highly order hydrogen-bonded surface layer of water and methanol were sheathing the ODS, then the observed hindered chain motion could be rationalized.

This proposed structure is also compatible with the present understanding of the microstructure of the methanol–water solvent. For solutions of methanol–water where the methanol concentration is significantly higher than that of water, such as the mixture used in this study, two different statistical mechanical simulations [31,32] predicted that hydrophobic solvation of the methanol molecules cause ca. sixteen self-associated water molecules to form a cage around the methyl portion of the alcohol; while the hydroxyl portion of the alcohol forms hydrogen bonds with only ca. 2.6 water molecules. Similar engagement of the C_{18} phase by associated water or a water–methanol sheath may be causing the observed low desorption rate constant for naphthalene and the interaction with ODS when solvated in the 2.3 methanol–water mole ratio eluent.

4.5. Time of analysis

In the previous section, improvements in efficiency were demonstrated. However, instead of simply improving efficiency of a separation, a more practical goal is to increase resolution per unit time and therefore decrease the time of analysis. If the time of analysis, t, is defined as the retention time of the last eluting peak, then Eq. 10 shows the relationship between experimentally controlled chromatographic variables and t for the separation of two analytes.

$$t = 16R_s^2 \cdot \left(\frac{\alpha}{\alpha - 1}\right)^2 \cdot \left(\frac{(1 + k')^3}{k^2}\right) \cdot \left(\frac{H}{u}\right) \qquad (10)$$

where t is time of analysis, R_s is resolution, α is separation factor, k' is capacity factor of the peak, H is the plate height and u is the mobile

phase linear velocity. Once the chromatographic system is chosen (stationary phase, solvent, solute, etc.), capacity factors and the separation factor are constants. Therefore, when R_s is fixed for a required separation, the ratio of H to u must be minimized to decrease time of analysis not H itself.

Fig. 8 shows the variation of H/u versus u for the methanol–water mixture and for the methanol–water mixture with 0.5 mole fraction CO_2 added for naphthalene. When methanol–water was the eluent, the H/u ratio reached a minimum value for a linear velocity of 0.15 cm/s or reduced linear velocity of ca. 5. The H/u ratio for the eluent with 0.5 mole fraction CO_2 does not reach a minimum until linear velocities of 0.4–0.5 cm/s are reached. Also, the mobile phase with 0.5 mole fraction CO_2 shorten the analysis time by factors of 2.5 and 8 at linear velocity of 0.15 ($\nu = 5$) and 0.35 ($\nu = 17$) cm/s, respectively. If a specific analysis time is required, the low H/u value at high velocity for the eluent with added CO_2 will allow longer column lengths to be used without losing resolution. Because the permeability of the column is much higher when CO_2 is added to the mobile phase, very long packed capillary columns should be possible at workable inlet pressures for the separation of highly complicated samples.
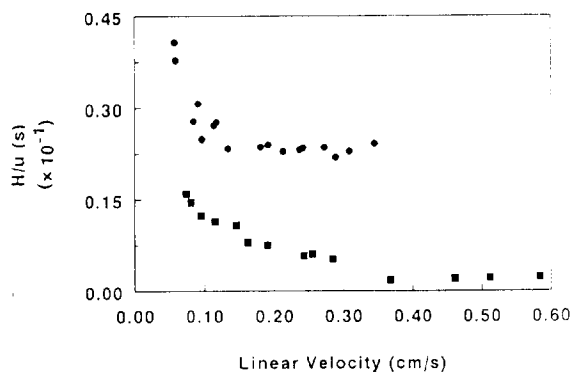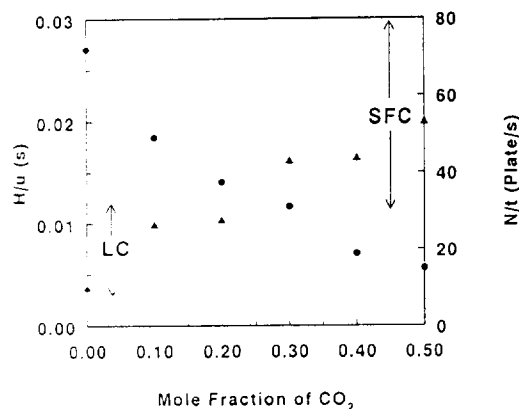

Fig. 9. Variation of observed number of plates per unit time, N/s (▲) and the ratio of plate height to the mobile phase linear velocity, H/u (●) with mole fraction of CO_2 in the mobile phase when the methanol–water mole ratio was maintained at 2.3. Vertical lines show typical N/s values in HPLC and SFC.

Finally, Fig. 9 shows the variation in the H/u and N/t (number of theoretical plates per unit time) ratios as a function of added CO_2 for naphthalene at a reduced linear velocity of 5. The range of N/t for standard packed HPLC and packed SFC with 5-μm particles is also marked [33]. Clearly, as expected the use of enhanced-fluidity mobile phases moves the measured N/t into a range larger than found in standard HPLC and common for SFC.

Acknowledgement

Fig. 8. Variation of the ratio of plate height to linear velocity with mole fraction of CO_2 in the mobile phase for naphthalene. ■ = 0.5 Mole fraction of CO_2 in the methanol–water–CO_2 mobile phase with the methanol–water mole ratio held at 2.3; ● = methanol–water mixture as mobile phase.

References

[1] Y. Cui and S.V. Olesik, Anal. Chem., 63 (1991) 1812.
[2] J. Timmermans, The Physico-Chemical Constants of Binary Systems in Concentrated Solutions, Vol. 4, Interscience, New York, 1960, p.162.
[3] J.H. Knox, J. Chromatogr. Sci. 15 (1977) 352.
[4] C.R. Wilke and P. Chang, AIChE J., 1 (1955) 264.
[5] L.R. Perkins and C.J. Geankoplis, Chem. Eng. Sci., 24 (1969) 1035.

[6] A.S. Teja and P. Rice, *Chem. Eng. Sci.*, 36 (1981) 7.

[7] A.S. Teja and P. Rice, *Ind. Eng. Chem. Fundam.*, 20 (1981) 77.

[8] P.C. Reid, J.M. Prausnitz and B.E. Poling, *The Properties of Gases and Liquids*, McGraw-Hill, New York, 4th ed., 1987, p. 480.

[9] K. Lucas, *Chem. Ing. Tech.*, 53 (1981) 959.

[10] K. Stephan and K. Lucas, *Viscosity of Dense Fluids*, Plenum Press, New York, 1979, p. 75.

[11] P.R. Sassiat, P. Mourier, M.H. Caude and R.H. Rosset, *Anal. Chem.*, 59 (1987) 1164.

[12] R.T. Kennedy and J.W. Jorgenson, *Anal. Chem.*, 61 (1989) 1128.

[13] T. Chang and R.W. Rousseau, *Fluid Phase Equilib.*, 23 (1985) 243.

[14] J.H. Knox, *J. Chromatogr. Sci.*, 18 (1980) 453.

[15] C.A. Cramers, J.A. Rijks and C.P.M. Schutjes, *Chromatographia*, 14 (1981) 439.

[16] C. Borra, M.H. Soon and M. Novotny, *J. Chromatogr.*, 385 (1987) 75.

[17] R. Ohmacht and I. Halász, *Chromatographia*, 14 (1981) 155.

[18] M.J. Kamlet, J.L.M. Abboud and R.W. Taft, *Prog. Phys. Org. Chem.*, 13 (1983) 485.

[19] W.J. Cheong and P.W. Carr, *Anal. Chem.*, 60 (1988) 820.

[20] P.C. Sadek, P.W. Carr, R.M. Doherty, M.J. Kamlet, R.W. Taft and M.H. Abraham, *Anal. Chem.*, 57 (1985) 2971.

[21] S.A. Wise and L.C. Sander, *J. High Resolut. Chromatogr. Chromatogr. Commun.*, 8 (1985) 248.

[22] K. Jinno and M. Okamoto, *Chromatographia*, 18 (1984) 495.

[23] L.R. Snyder and J.J. Kirkland, *Introduction to Modern Liquid Chromatography*, Wiley, New York, 2nd ed., 1979, p. 836.

[24] K.-E. Karlsson and M. Novotny, *Anal. Chem.*, 60 (1988) 1662.

[25] B.L. Karger, M. Martin and G. Guiochon, *Anal. Chem.*, 46 (1974) 1640.

[26] Cs. Horváth and H.-J. Lin, *J. Chromatogr.*, 126 (1976) 401.

[27] Cs. Horváth and H.-J. Lin, *J. Chromatogr.*, 149 (1978) 43.

[28] R.P.W. Scott and P. Kucera, *J. Chromatogr.*, 169 (1979) 51.

[29] C.R. Yonker, T.A. Zwier and M.F. Burke, *J. Chromatogr.*, 241 (1982) 257.

[30] M.E. Gangoda and R.K. Gilpin, *Langmuir*, 6 (1990) 941.

[31] W.L. Jorgensen and J.D. Madura, *J. Am. Chem. Soc.*, 105 (1983) 1407.

[32] M. Ferrario, M. Haughney, I.R. McDonald and M.L. Klein, *J. Chem. Phys.*, 93 (1990) 5156.

[33] M.L. Lee and K.E. Markides (Editors), *Analytical Supercritical Fluid Chromatography and Extraction*, Chromatography Conferences, Provo, UT, 1990, p. 27.